Progress In Electromagnetics Research, PIER 84, 307–319, 2008

HIGH IMPEDANCE GROUND PLANE (HIGP) INCORPORATED WITH RESISTANCE FOR RADAR CROSS SECTION (RCS) REDUCTION OF ANTENNA

Q.-R. Zheng, Y.-M. Yan, X.-Y. Cao, and N.-C. Yuan

Telecommunication Engineering College
Airforce Engineering University
Xi'an 710077, P. R. China

Abstract—In this paper a novel ultra-thin radar absorbent material (RAM) using HIGP is presented and investigated. Owing to the high impedance property of the HIGP, the thickness of the RAM is about several tenths of the centre wavelength of the absorption band, considerably thinner than conventional absorbers. The absorption band of the RAM is about several hundred megahertz. In the new RAM, lumped resistances are soldered between the patches of mushroom-like high-impedance surface (HIGP). And the metal ground plane of waveguide slot antenna is covered by this new type of RAM. As compared to the slot antenna with a metal ground plane, the measured results show that the radar cross section (RCS) of waveguide slot antenna reduces significantly. This proves that the new HIGP RAM has a good radar absorbing characteristics. The simulations and experiment results have shown that the RCS of antenna is reduced by 7.9 dB and gain is only reduced by 0.9 dB.

1. INTRODUCTION

HIGP are a kind of artificial electromagnetic materials that are typically realized by periodic metallic patterns arranged on dielectric substrates, and have electromagnetic characteristics that differ with the patterns, such as negative refraction [1–5], electromagnetic bandgap [6–9], and high-impedance properties [10–12]. Of all the interesting properties, the high-impedance feature is of particular interest. As a potential application of the feature, Engheta has described an idea of the possibility of having thin absorbing screens using metamaterial surfaces [13, 14]. Kern and Werner have designed ultra-thin absorbers by using high-impedance frequency-selective

surfaces (HZ FSS) [15]. However, the patterns of HZ FSS designed by them using a genetic algorithm are rather complex and difficult to engineer. Valagiannopoulos had studied the coating which can optimize the RCS of the perfectly conducting circular cylinder, but the method which is employing Greens functions integral is very complex also [16]. In this paper, a novel ultra-thin RAM using the Sievenpiper HIGP is presented. The new-style RAM takes the form of the Salisbury screen, which is a famous kind of RAM, and the ultra-thin design is based on the high-impedance properties of the HIGP. Two application examples, including waveguide end-slot antenna and asymmetric waveguide slot antenna, with and without HIGP RAM, have been presented to suggest that the new type of RAM is potentially useful in antenna field for RCS reduction.

2. STRUCTURE OF THE ULTRA-THIN RAM BASED ON HIGP

2.1. Structure of HIGP RAM

An ultra-thin electromagnetic absorber is presented, which is composed of lumped resistances and a Sievenpiper HIGP, as shown in Fig. 1. The HIGP typically consists of a periodic array of metal plates, connected to a solid metal ground by vertical conducting vias. The top view and the profile of the HIGP are shown in Fig. 1(a).

Since the HIGP is lossless in the microwave regime, the reflection coefficient of the HIGP can be set as:

$$R_1 = \exp(j\phi) \tag{1}$$

where ϕ is the reflective phase of the HIGP, which is defined as the phase difference of the reflection field and the incident field at the reflecting surface, and changes continuously from π to $-\pi$ with the frequency of the incident wave increasing. Obviously, there exists a resonance frequency at which the reflection phase is zero, which suggests that the HIGP surface behaves like an artificial magnetic conductor. Far below the resonant frequency, the phase is π and the surface is just like an ordinary metal surface. Above the resonance frequency, the phase approaches $-\pi$ asymptotically. Fig. 1(b) shows the geometry of the ultra-thin absorber. The HIGP is placed on the shielded surface, and the lumped resistances are soldered between the patches of HIGP. Fig. 1(c) shows the equivalent circuit model of the ultra-thin absorber. From the recursive relation for the reflective coefficient of the Salisbury screens derived in [17–19], the reflection

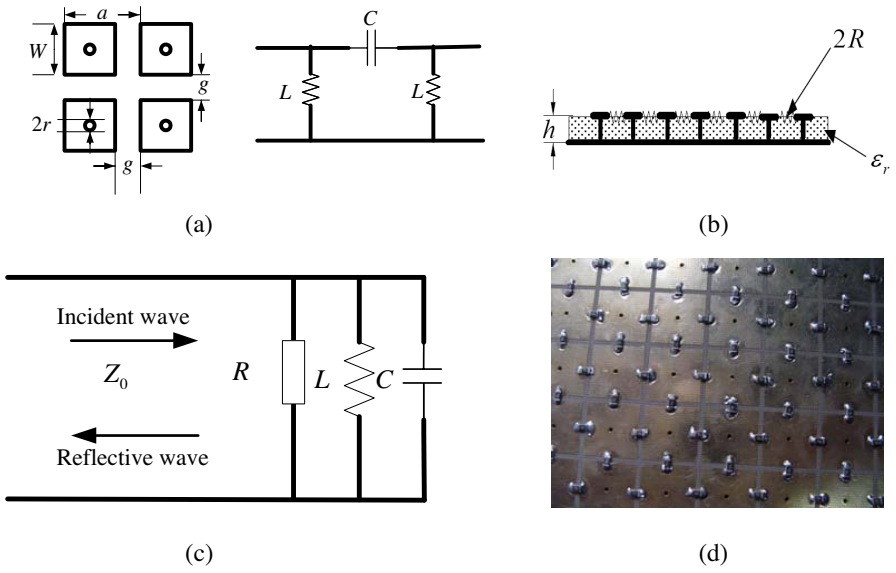

Figure 1. Ultra-thin electromagnetic absorber. (a) Top view and cross-section of HIGP. (b) Geometry of ultra-thin absorber. (c) Equivalent circuit model of ultra-thin absorber. (d) Practical ultra-thin absorber.

coefficient of the ultra-thin absorber can be obtained as:

$$\begin{aligned} R_2 &= \frac{-(1-R_1)}{2(1+R_1)+(1-R_1)} \\ \frac{1}{R_2} &= -1 - j\frac{2}{tg(\phi/2)} \end{aligned} \tag{2}$$

Then the power reflection coefficient of the ultra-thin absorber is

$$R_P = |R_2|^2 = \frac{tg^2(\phi/2)}{4+tg^2(\phi/2)} \tag{3}$$

Figure 2 shows the function plot of (3). It can be shown that R_p reaches a minimum at $\phi = 0$, and the absorption deteriorates rapidly when f increases. However, ϕ is a nonlinear function of the frequency of the incident wave, and the region between $-\pi/2$ and $\pi/2$ corresponds to the forbidden frequency band of the HIGP. So a broad absorption band can be expected if a proper HIGP with a broad forbidden frequency band is designed.

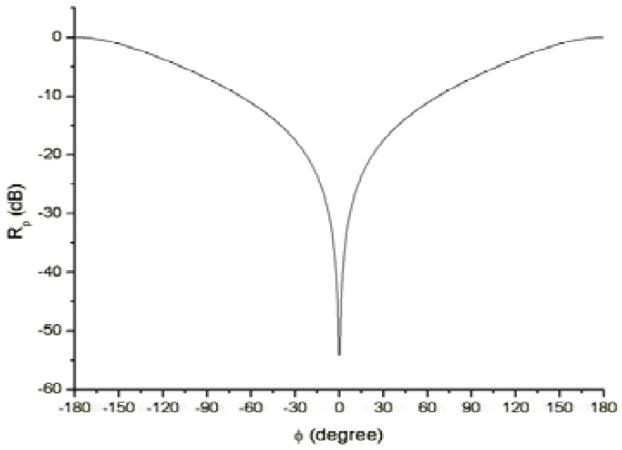

Figure 2. Dependence of power reflection coefficient on reflection phase of HIGP.

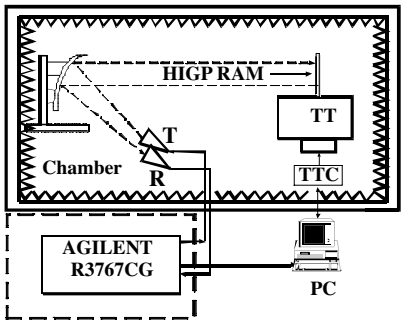

Figure 3. Testing system of HIGP RAM.

2.2. Testing system of HIGP RAM

The testing system of HIGP RAM is shown in Fig. 3. It consists of network analyzer, horn antenna, amplifier, and so on. The testing principle is this: "T" denotes the transmitting antenna. It transmits electromagnetic wave which is produced by network analyzer, and the electromagnetic wave is reflected by the reflector antenna and changed to be plane wave. The plane wave is received by the receiving antenna which is plot as "R" shown in the Fig. 3. The testing procedure need twice. The first time is to test the property of metal ground plane. Its magnitude is $\mathrm{Mag}(\Gamma_{metal})$(dB), and phase is $\mathrm{Arg}(\Gamma_{metal})$; the second time is to test HIGP RAM. Its magnitude is $\mathrm{Mag}(\Gamma_{HIGPRAM})$(dB),

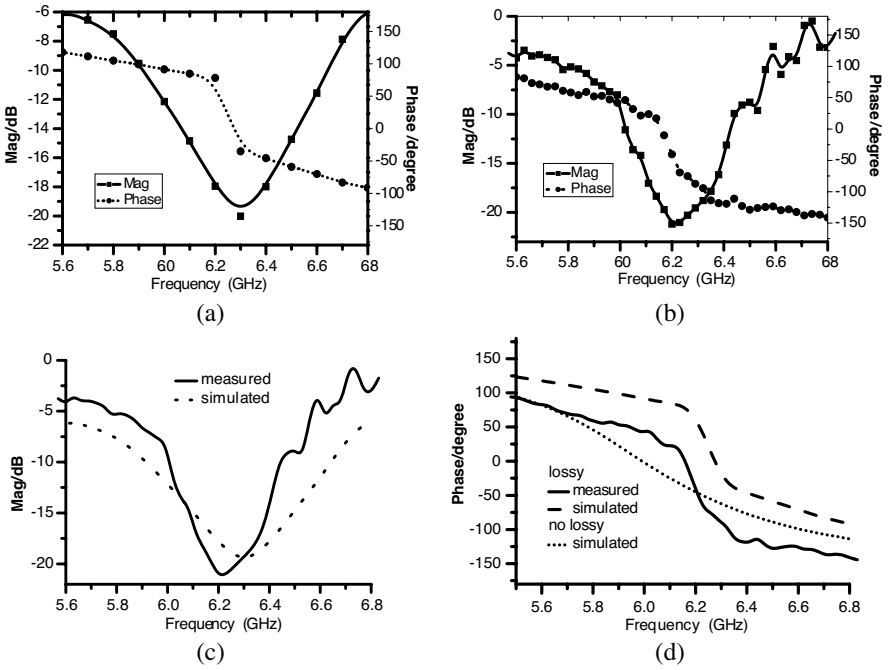

Figure 4. Reflection coefficient of ultra-thin absorber. (a) Simulated reflection coefficient. (b) Measured reflection coefficient. (c) Comparison of magnitude. (d) Comparison of phase.

and the phase is $\mathrm{Arg}(\Gamma_{HIGPRAM})$. The differences of the two testing results:

$$\mathrm{Mag}(\Gamma)(\mathrm{dB}) = \mathrm{Mag}(\Gamma_{metal})(\mathrm{dB}) - \mathrm{Mag}(\Gamma_{HIGPRAM})(\mathrm{dB}) \quad (4)$$

$$\mathrm{Arg}(\Gamma) = \mathrm{Arg}(\Gamma_{HIGPRAM}) - \mathrm{Arg}(\Gamma_{metal}) - 180^{\circ}] \quad (5)$$

The modified formula (4) and (5) are the actual magnitude and phase of HIGP RAM. And in the testing system, some absorbing materials are need to place between the transmitting and receiving antenna in order to reduce the coupling between the two antennas.

In this Section, we consider an HIGP with the following parameters: $a = 7.2\,\mathrm{mm}$, $W = 6.8\,\mathrm{mm}$, $r = 0.4\,\mathrm{mm}$, $g = 1\,\mathrm{mm}$, $h = 1.5\,\mathrm{mm}$ and $\varepsilon_r = 2.65$. The lumped resistance $R = 375\,\Omega$. The absorption property of the ultra-thin absorber using the HIGP is shown in Fig. 4. It can be seen that the electromagnetic wave is absorbed in the region 6.0–6.6 GHz, corresponding to an absorption bandwidth of about 600 MHz. The absorption reaches a maximum at

$f_0 = 6.3\,\text{GHz}$, which corresponds to a wavelength $\lambda_0 = 4.72\,\text{cm}$. Since the lossy screen is very thin, the depth of the absorber is the same as that of the HIGP, much less than the wavelength: $h/\lambda_0 \approx 0.031$. The measured results basically agree well with the simulated results. There are only small errors between simulated and measured results. This is due to the following: one hand the calculating model is based on the infinite periods HIGP, and the actual HIGP is finite in size; on the other hand, some inductive parasitics can be produced when the resistors are soldered on the surface of HIGP. And from Fig. 4d it can be found that the bandwidth of the ultra-thin absorber is decided by the bandgap of the HIGP. The errors produced by some inductive prasitics of resistors are not very evident.

3. APPLICATION OF HIGP RAM IN RADAR ANTENNA FOR RCS REDUCTION

Radar antenna system usually produces very big RCS at its normal direction on the airborne. For example, the RCS of Cassegrain antenna on a typical X band missile often can reach to 10 dBsm; and for the waveguide slotted antenna array which is used in Pulse Doppler Radar, its RCS often can reach to 30 dBsm. Thus how to reduce the antenna system's RCS has become a crucial problem in the target stealth technology. But owing to the antenna's working features: one hand it must ensure the radar can receive and transmit electromagnetic wave normally, and on the other hand the antenna's RCS must be reduced. This has become a crucial problem which is very difficult to be solved in the stealth technology.

Because the lumped resistances are soldered on the HIGP surface, and the thickness of the whole structure is ultra thin, the structure can be embeded in antenna array and cannot affect the antenna's performance obviously.

3.1. RCS Reduction in Waveguide End-slot Antenna

As shown in the Fig. 5, the antenna is with (a) metal ground plane and (b) HIGP RAM. The HIGP structure and Material are the same as in Fig. 4. In the region 6.0–6.6 GHz, the electromagnetic wave is absorbed, and the absorption reaches to $-22\,\text{dB}$ at $f_0 = 6.3\,\text{GHz}$. The antenna's parameters are: slot length $L = 24\,\text{mm}$, width $W = 2\,\text{mm}$. the parameters of feeding waveguide are: broad wall $a = 40.4\,\text{mm}$, narrow wall $b = 20.2\,\text{mm}$. In order to lead the electromagnetic wave to radiate into the outer space as much as possible and reduce the coupling between the RAM and the slot at the same time, some space

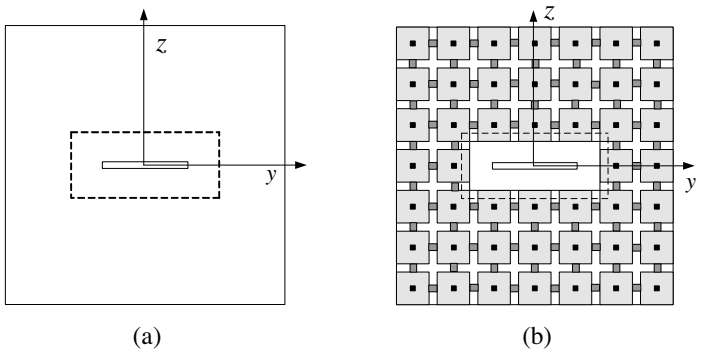

Figure 5. Configuration of waveguide end-slot antenna (a) with metal ground plane (b) with HIGP RAM.

between them must be left.

1) Calculating Method

The FDTD based on Perfect Match Layer (PML) are used to prove our ideas. Because confined by the computer's resource, we only calculate the structure shown in the Fig. 5. Three periods of HIGP are placed at the up and down side of the waveguide slot antenna, respectively; and on the left and right section are two periods. The antenna is placed on the *yoz* plane.

2) Simulated results and discussion

(1) Return loss parameters

As shown in Fig. 6, the return loss parameter (S11) keeps very well after loading HIGP RAM, and this indicating that the spacing between HIGP RAM and slot is appropriate. Owing to the coupling results from the slot and HIGP, the resonant frequency moves to lower frequency. This can be solved by enlarging the spacing in order to reduce the coupling between them or adjusting the length of radiating slot.

(2) Antenna radiation pattern

From the Fig. 6, it can be seen that the two antennas S11 parameters have the same values at 6.09GHz which are -25.6 dB. Fig6 shows the measured radiation patterns of the antenna with HIGP RAM and another with conventional metal ground plane of the same size. The two antennas work at the same frequency (6.09 GHz) because they have the same input power at this frequency.

From the Fig. 7, it can be seen that the ripples on the antenna pattern become more obvious, especial in H plane, than that with metal

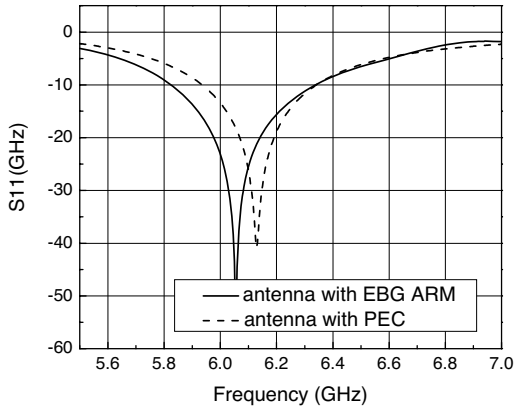

Figure 6. Simulated return loss of waveguide end-slot antenna.

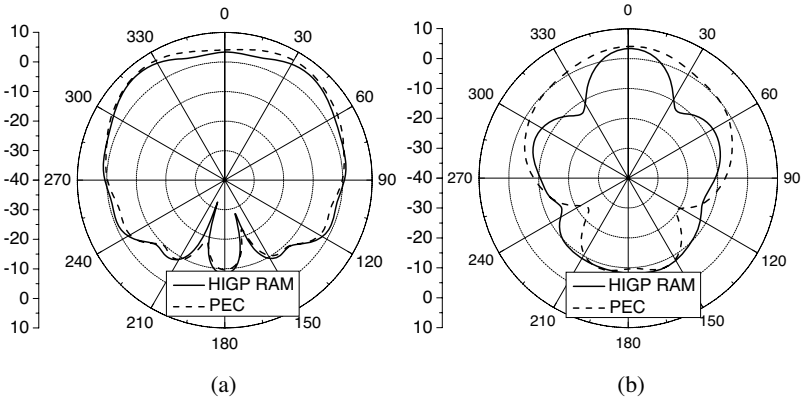

(a) (b)

Figure 7. Simulated radiation pattern of waveguide end-slot antenna (a) E-plane. (b) H-plane.

ground plane. The gain reduced by 0.8 dB, and the back lobe does not reduce. This is because the HIGP RAM can not suppress the surface wave of the antenna, and accordingly it cannot reduce the diffraction of the electromagnetic wave at the corner of antenna. Thus the back lobe of the antenna cannot be improved after loading HIGP RAM.

(3) RCS reduction

From the Fig. 8, the Max RCS of waveguide end-slot antenna with HIGP RAM is -10 dBsm, and is reduced by 4.53 dB than the original one. The simulation results suggest that no matter what polarization the incident electromagnetic wave is, the antenna with HIGP RAM both have the lower RCS value at the normal direction. And at the

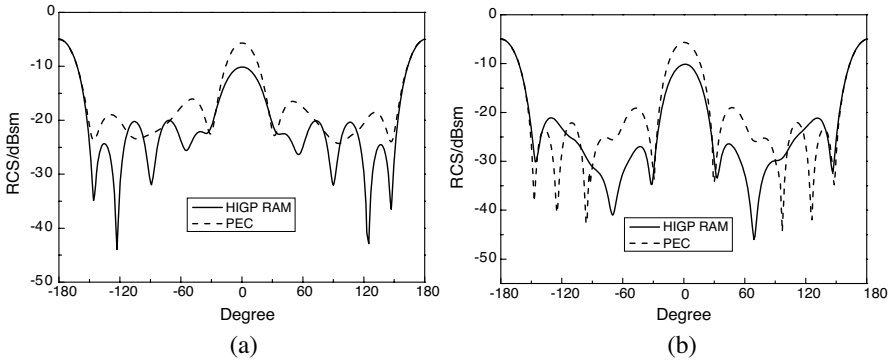

Figure 8. Simulated RCS of waveguide end-slot antenna, (a) horizontal polarization, (b) vertical polarization.

backward direction, the antenna with and without HIGP RAM have the same RCS. This is because the two antennas have the same metal ground at the backward direction.

3.2. RCS Reduction in Asymmetric Waveguide Slot Antenna Array

Asymmetric waveguide slot antenna is a common radiation unit, especially in radar and communication system. The applications of HIGP in waveguide slot antenna have been studied in recent years [20–22], the conclusions show that the HIGP has a few benefits to antenna: the pattern of the slot antenna is improved, the back lobes are reduced and the gain is increased. But merely no attention is paid on the RCS of slot antenna with HIGP.

The configuration of the waveguide slot antenna array with HIGP RAM is shown in Fig. 9. It consists of two parts: HIGP RAM and a 4×10 waveguide slot antenna array. The ground plane of antenna is covered by HIGP RAM. For the HIGP RAM used in slot antenna, the metal patch size is 10×10 mm, and the gap between the patches is 0.2 mm. The substrate is 3 mm thick with relative permittivity 3.5. The electromagnetic wave is absorbed in the region 3.06–3.68 GHz, The working frequency of slot antenna arrays is 3.35 GHz which is within the band-gap of HIGP.

The radiation patterns of the two antennas are measured in an anechoic chamber and shown in Fig. 10. The results suggest that the two radiation patterns are similar to each other as a whole and the gain of antenna with HIGP RAM decreased about 1 dB than that with metal ground plane.

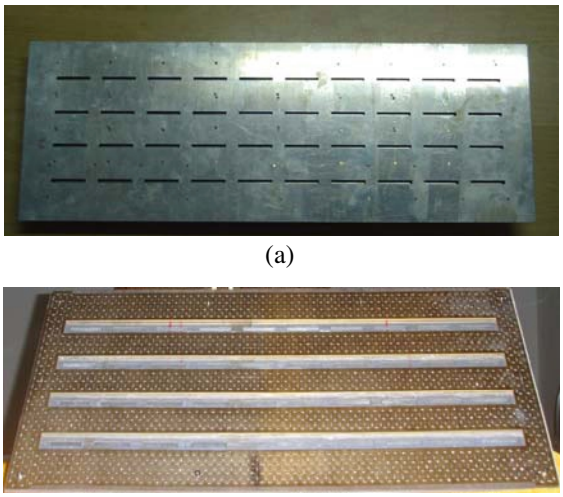

(a)

(b)

Figure 9. Photograph of the waveguide slot antenna with (a) metal ground plane, (b) HIGP RAM.

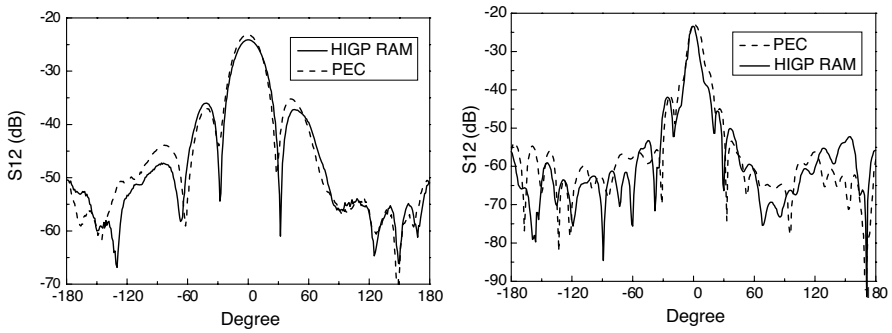

(a) (b)

Figure 10. Measured radiation pattern of waveguide end-slot antenna (a) E-plane, (b) H-plane.

The RCS of the two slot antenna arrays are measured also. For the incident wave with horizontal polarization, the measured RCS of two antennas are shown in Fig. 11(a). The RCS of antenna decreases about 8 dB from -5° to 5° than that of slot antenna without HIGP RAM. And for the incident with vertical polarization, the RCS of two antennas are shown in Fig. 11(b). RCS decreases about 8 dB at main lobe. Because the coupling between slots in the E-plane is much higher

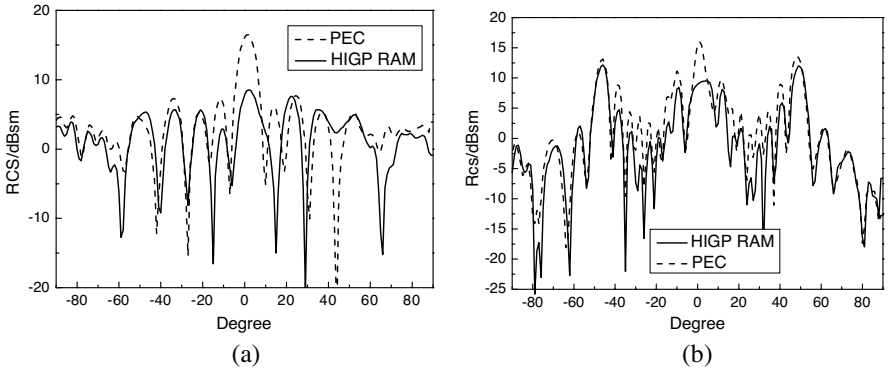

Figure 11. Measured RCS of waveguide end-slot antenna, (a) horizontal polarization, (b) vertical polarization.

than that in the H-plane [19, 20], the configuration of HIGP is designed mainly for the E-plane. Reduction effect for E-plane is better than for H-plane.

4. CONCLUSIONS

A novel RAM which is designed by using the Sievenpiper HIGP is shown in this paper. The absorption performance of the RAM is determined by the high-impedance property of the HIGP, so that the expected absorption band can be obtained by regulating the HIGP. And a waveguide slot antenna with the new RAM has been proposed. The simulated and measured results show that the RCS of the slot antenna with HIGP RAM reduced obviously at normal direction. These reductions can be attributed to the radar absorbing characteristics of HIGP RAM. So the new type of HIGP RAM can be considered as a new radar absorbing material.

ACKNOWLEDGMENT

This work is supported partially by Natural Science Foundation of China under contract No. 60401011 and No. 60401001.

REFERENCES

1. Zharov, A. A., I. V. Shadrivov, and Y. S. Kivshar, "Nonlinear properties of left-handed metamaterials," *Phys. Rev. Lett.*, Vol. 91, 037401, 2003.

2. Yang, R., Y.-J. Xie, P. Wang, and L. Li, "Microstrip antennas with left-handed materials substrates," *J. of Eletromagn. Wave and Appl.*, Vol. 20, No. 9, 1235–1248, 2006.
3. Li, Z. and T. Cui, "Novel waveguide directional couplers using left-handed materials," *J. of Eletromagn. Wave and Appl.*, Vol. 21, No. 8, 1053–1062, 2006.
4. Srivastava, R., S. Srivastava, and S. P. Ojha, "Negative refraction by photonic crystal," *Progress In Electromagnetics Research B*, Vol. 2, 15–26, 2008.
5. Abdalla, M. A. and Z. Hu, "On the study of left-handed coplanar waveguide coupler on Ferrite\R\Nsubstrare," *Progress In Electromagnetics Research Letters*, Vol. 1, 69–75, 2008.
6. Sievenpiper, D., et al., "High-impedance electromagnetic surface with a forbidden frequency band," *IEEE Trans. Microw. Theory Tech.*, Vol. 47, No. 11, 2059–2074, 1999.
7. Zheng, Q.-R., Y.-Q. Fu, and N.-C. Yuan, "Characteristics of plannar PBG structures With a cover layer," *J. of Eletromagn. Wave and Appl.*, Vol. 20, No. 11, 1439–11453, 2006.
8. Li, L., C.-H. Liang, and C. H. Chan, "Waveguide end-slot phased array antenna integrated with electromagnetic bandgap structure," *J. of Eletromagn. Wave and Appl.*, Vol. 21, No. 2, 161–174, 2007.
9. Zheng, Q.-R., B.-Q. Lin, and N.-C. Yuan, "Characteristics and applications of a novel compact spiral electromagnetic bandgap (EBG) structure," *J. of Eletromagn. Wave and Appl.*, Vol. 21, No. 2, 199–213, 2007.
10. Yang, F. and Y. Rahmat-Samii, "Reflection phase characterizations of the HIGP ground plane for low profile wire antenna applications," *IEEE Trans. Antennas Propag.*, Vol. 51, 2691–2703, 2003.
11. Sievenpiper, D., "High-impedance electromagnetic surfaces," Ph.D. Thesis, University of California, Los Angeles, 1999.
12. Zhang, G.-H. and N.-C. Yuan, "Radiation characteristics improvement in waveguide-fed slot antenna with a high-impedance ground plane," *Microwave and Optical Technology Letters*, Vol. 45, No. 2, 176–179, 2005.
13. Engheta, N., "Thin absorbing screens using metamaterial surfaces," *IEEE Antennas and Propagation Society (AP-S), Int. Symp. and USNC National Radio Science Meeting*, 16–21, San Antonio, TX, USA, 2002.
14. Alu and Engheta, "Achieving transparency with plasmonic and

metamaterial coatings," *Phys. Rev. E*, Vol. 72, 016623, 2005.

15. Kern, D. J. and D. H. Werner, "A genetic algorithm approach to the design of ultra-thin electromagnetic bandgap absorbers," *Microwave and Optical Technology Letters*, Vol. 38, No. 1, 61–64, 2003.
16. Valagiannnopoulos, "Arbitrary currents on circular cylinder with inhomogeneous cladding and RCS optimization," *J. of Eletromagn. Wave and Appl.*, Vol. 21, No. 5, 665–680, 2007.
17. Fante, R. L. and M. T. McCormack, "Reflection properties of the Salisbury screen," *IEEE Trans. Antennas Propag.*, Vol. 36, 1443–1454, 1988.
18. Vinoy, K. J. and R. M. Jha, "Radar absorbing materials: From theory to design and characterization," Kluwer Academic, Boston, MA, 1996.
19. Salisbury, W. W., "Absorbent body for electromagnetic waves," US Patent, 2 599 944, June 10, 1952.
20. Zheng, Q.-R., G.-H. Zhang, and N.-C. Yuan, "Single ridged waveguide slot phased antenna array integrated with high impedance ground plane," *APMC2005 Proceedings*, 2005.
21. Li, L., X.-J. Dang, B. Li, and C.-H. Liang, "Analysis and design of waveguide slot antenna array integrated with electromagnetic band-gap structures," *IEEE Antennas and Wireless Propagation Letters*, Vol. 5, No. 12, 111–115, 2006.
22. Li, B., B. Wu, and C.-H. Liang, "High gain circular waveguide array antenna using electromagnetic bandgap structure," *J. of Eletromagn. Wave and Appl.*, Vol. 20, No. 7, 955–966, 2006.